Desalination and Water Treatment
www.deswater.com
doi: 10.1080/19443994.2015.1025849

57 (2016) 8754–8764
April

Taylor & Francis
Taylor & Francis Group

Removal of boron from aqueous solution using magnesite and bentonite clay composite

Vhahangwele Masindi[a,b,*], Mugera W. Gitari[a], Hlanganani Tutu[c], Marinda Debeer[d]

[a]*Department of Ecology and Resources Management, University of Venda, P/Bag X5050, Thohoyandou 0950, South Africa, Tel. +27 0128414107; emails: VMasindi@csir.co.za, masindivhahangwele@gmail.com (V. Masindi), Tel. +27 0159628572; email: Mugera.gitari@univen.ac.za (M.W. Gitari)*
[b]*CSIR (Council of Scientific and Industrial Research), Built Environment, Building Science and Technology (BST), P.O. Box 395, Pretoria 0001, South Africa*
[c]*Molecular Sciences Institute, School of Chemistry, University of the Witwatersrand, P/Bag X4, WITS, 2050 Johannesburg, South Africa, Tel. +27 0117176771; email: Hlanganani.tutu@wits.ac.za*
[d]*DST/CSIR National Centre for Nano-structured Materials, Council for Scientific and Industrial Research, P.O. Box 395, Pretoria 0001, South Africa, Tel. +27 0128414107; email: mdebeer@csir.co.za*

Received 3 June 2014; Accepted 28 February 2015

ABSTRACT

The removal of boron from industrial effluents using the composite was studied in batch equilibration technique. The effects of equilibration time, adsorbent dosage, concentration and pH on removal of boron were investigated. The experiments demonstrated that boron removal is optimum at 30 min of agitation, 1 g of dosage and 20 mg L^{-1} of ion concentration. Adsorption of boron by the composite was independent of pH. The adsorption data fitted well into both Langmuir adsorption isotherm and Freundlich adsorption isotherm hence proving monolayer and multilayer adsorption. The kinetic studies reported that the data favours pseudo-second-order reaction than first order hence proving chemisorption. Under optimized conditions, the composite was able to remove boron to below World Health Organization (WHO) water quality guidelines. Henceforth, it was concluded that this comparative study will be helpful for further application in the treatment of boron-contaminated water.

Keywords: Bentonite clay; Magnesite; Composite; Boron; Kinetics; Adsorption

1. Introduction

World Health Organisation (WHO) recommends 0.5 mg L^{-1} of boron in drinking water [1,2]. Intake of excessive levels of boron may lead to the development of prostaglandins, leukotriene, premature menopause, birth pathology, testicular atrophy and degeneration, changes neurological effects, physical disorders and intellectual development of children, rheumatoid arthritis, prostate cancer, menopausal osteoporosis and inflammatory effects [3–8]. Boron has narrow deficiency and excess range hence making it toxic to living organisms [9–20].

Pollution of the environment by boron is caused by man-made activities and weathering of the natural environment accounts for total boron in water bodies [4–6,8,21]. Speciation and adsorption of boron in the

*Corresponding author.

environment is pH dependent. The species of boron are boric acid [$B(OH)_3$] at low pH and borate [$B(OH_4^-)$] at alkaline pH conditions [1,22]. Considering high mobility and toxicity of boron in the environment, serious mitigation measures need to be developed and implemented. Boron has to be contained and removed from wastewater before environmental contamination. A number of passive and active technologies have been developed and implemented for decontamination of boron-rich water and they include: phytoremediation [23], constructed wetlands [24], adsorption [25], precipitation [1,26], reverse osmosis [27] ion exchange [16], coagulation [28] and desalination [9,29]. Amongst them, adsorption followed by precipitation has been regarded the best treatment technology [9,11,13,14,16,22,25,26,30–32]. This study was therefore designed to remove boron from industrial effluents using cryptocrystalline magnesite and bentonite clay composite. Yellow Star Quarries in the Kroonstad district, Cape Town, RSA contains 750,000 m^3 deposit of bentonite that can be projected to 67 years if it is mined at a rate of 4,000 m^3 $month^{-1}$. Magnesite mine in Folovhodwe, Limpopo province, RSA showed that the magnesite deposit is close to 18 mega tons of amorphous magnesite, which can be mined for the coming 50 years [33]. In terms of economic viability, the technology will be feasible since it is relying on natural and locally available materials.

2. Materials and methods

2.1. Adsorbent

Raw magnesite rocks were collected prior any processing at the mine from the Folovhodwe Magnesite Mine in Limpopo Province, South Africa (22˚35´´47.0´´ S and 30˚25´33´´E). Magnesite samples were milled to a fine powder using a Retsch RS 200 miller and passed through a 32 μm particle size sieve. Raw AMD samples were collected from a disused mine shaft in Krugersdorp, Gauteng Province, South Africa. Bentonite clay samples were supplied by Bentonite PTY, LTD (Cape Town, South Africa). The raw bentonite samples were washed by soaking the samples in ultrapure water and draining the water after 10 min. The ultrapure water used was such that it covered the entire sample in the beaker and allowed to overflow. The procedure was repeated four times. The washed bentonite was then dried in an oven for 24 h at 105˚C. The dried samples were crushed into a fine powder using a Retsch RS 200 miller and passed through a 32 μm particle size sieve. Thereafter, the composite (1 kg) of powdered bentonite and magnesite was fabricated on 1:1 g ratio. Five hundred gram of bentonite clay was mixed with 500 g of magnesite. The mixtures were crushed and homogenized by pulverizing them together into fine powder using a Retsch RS 200 miller (USA) and passed through a 32 μm particle size sieve. After sieving, the samples were tightly kept in zip lock plastic bags until application for wastewater amelioration.

2.2. Preparation of working solution

1,000 mg L^{-1} standard solution of boron from Lab Consumables Supply, South Africa was used to prepare the working solutions. 10 mg L^{-1} working solution was prepared by extracting 10 mL of 1,000 mg L^{-1} standard solution and transferring into a 1,000 mL volumetric flask. The volumetric flask was topped to the mark by adding ultrapure water.

2.3. Characterization

Elemental analysis of raw and processed water samples was done by inductively coupled mass spectrometry (ICP-MS) (ELAN 6000). The accuracy of the analysis was monitored by analysis of National Institute of Standards and Technology (NIST) water standards. pH was monitored using CRISON MM40 portable pH/EC/TDS/Temperature multimeter. Chemical characteristics of magnesite samples were ascertained using X-ray fluorescence spectroscopy (XRF). Mineralogical characteristics of magnesite samples were ascertained using a Philips X-ray diffractometer with Cu-Kα radiation. Phase identification was performed by searching and matching obtained spectra with the powder diffraction file database with the help of Joint Committee of Powder Diffraction Standards (JCPDS) files for inorganic compounds (both XRF and X-ray diffraction (XRD) analysis were done at the facility of Geology, University of Pretoria). Surface analyses, chemical analysis and imaging on a variety of materials were performed using a scanning electron microscope coupled with energy dispersive spectrometer. Surface area was measured by Brunauer–Emmett–Teller (BET) equation (BET: A Tristar II 3020, Micrometrics BET from Norcross, GA, USA). pH_{pzc} was determined using solid addition method as described by Kumar et al. [34].

2.4. Experimental protocols

Optimization experiments were done in batch experimental procedures. Parameters optimized include time, dosage, boron concentration and pH. To evaluate effect of equilibration time on reaction

kinetics, time was varied from 0 to 360 min (10 mg L^{-1} boron, 1 g composite, 250 rpm, pH 11 and 26°C). To evaluate effect of dosage on reaction kinetics, the dosage was varied from 0.1 to 8 g (10 mg L^{-1} boron, 250 rpm, pH 11, 30 min of reaction time and 26°C). Boron removal with respect to ion concentration was conducted over a range of 0.1–60 mg L^{-1}. To evaluate effect of pH on removal of boron, the pH was varied from 2 to 12. A table shaker was used for all the experiments (1300E, Labcon, Petaluma, CA, USA). Optimized condition for testing the feedstock capacity to remove boron was evaluated using raw mine effluents.

2.5. Modelling

2.5.1. Percentage removal

The percentage removals of boron by the composite are computed by the expression:

$$\% \text{ Removal} = \left(\frac{C_0 - C_e}{C_0}\right) \times 100 \quad (1)$$

where C_0—initial concentration and C_e—equilibrium ion concentration, respectively.

2.5.2. Adsorption capacity

The grams of boron adsorbed by the composite are determined by the expression:

$$q = \frac{(C_i - C_e)V}{m} \quad (2)$$

where C_i—initial ion concentration (mg L^{-1}), C_e—ion concentration at equilibrium (mg L^{-1}), V—volume of ion solution (L) and m—weight of magnesite (adsorbent) (g).

2.5.3. Adsorption isotherms

The relationship between the amount of ions adsorbed and the ion concentration remaining in solution is described by an isotherm. The two most common isotherm types for describing this type of system are Langmuir and Freundlich adsorption isotherms. These models describe adsorption processes on a homogeneous (monolayer) or heterogeneous (multilayer) surface, respectively. The most important model of monolayer adsorption came from Langmuir. This isotherm is given as follows:

$$\frac{C_e}{q_e} = \frac{1}{Q_m b} + \frac{C_e}{Q_m} \quad (3)$$

The essential characteristics of the Langmuir isotherms can be expressed in terms of a dimensionless constant separation factor or equilibrium parameter, R_L, which is defined as:

$$R_L = \frac{1}{1 + bC_0} \quad (4)$$

$R_L > 1$ unfavourable
$R_L = 1$ linear
$0 < R_L < 1$ favourable
$R_L = 0$ irreversible
where C_e—equilibrium concentration (mg L^{-1}), Q_e—amount adsorbed at equilibrium (mg g^{-1}), Q_m—Langmuir constant related to adsorption capacity (mg g^{-1}) and b—Langmuir constant related to energy of adsorption (L mg^{-1}). A plot of C_e vs. C_e/Q_e should be linear if the data are described by the Langmuir isotherm. The value of Q_m is determined from the slope and the intercept of the plot. It is used to derive the maximum adsorption capacity and b is determined from the original equation and it represents the intensity of adsorption.

The Freundlich adsorption isotherm describes the heterogeneous surface energy by multilayer adsorption. The Freundlich isotherm can be formulated as follows:

$$\log\ q_e = \frac{1}{n}\log C + \log K \quad (5)$$

where C_e—equilibrium concentration (mg L^{-1}), q_e—amount adsorbed at equilibrium (mg g^{-1}), K—partition coefficient (mg g^{-1}) and n—intensity of adsorption. The linear plot of log C_e vs. log q_e indicates that the data are described by Freundlich isotherm. The value of K implies that the energy of adsorption on a homogeneous surface is independent of surface coverage and n is an adsorption constant which reveals the rate at which adsorption is taking place. These two constants are determined from the slope and intercept of the plot of each isotherm. An error analysis is required in order to evaluate the fit of the adsorption isotherms to experimental data. In the present study, the linear coefficient of determination of (R^2) was employed for the error analysis. The linear coefficient of determination is calculated using the equation:

$$r = \frac{n\sum xy - (\sum x)(\sum y)}{\sqrt{n(\sum x^2) - (\sum x)^2} - \sqrt{(\sum y^2) - (\sum y)^2}} \quad (6)$$

Theoretically, the R^2 value varies from 0 to 1. The R^2 value shows that the variation of experimental data is explained by regression equation. The coefficient of determination R^2 was applied to determine the relationship between the experimental data and the isotherms in most studies.

3. Results and discussion

3.1. X-ray fluorescence analysis

The elemental composition of bentonite clay, magnesite and composite is shown in Table 1.

Bentonite clay is dominated by Si and Al hence the name aluminosilicate [35]. There are traces of Fe, Mg, Ca, Na, K and Mn, respectively. The presence of Mg, Ca, Na and K indicate that these are exchangeable cations on the clay fractions. Magnesite showed the presence Mg as the major element. Traces of Ca, Si, Fe, Al and K were also observed on magnesite matrices. These results are consistent to results obtained by Zachamann and Johannes [36]. The composite was observed to contain Si, Mg and Al in significant amounts hence showing that this is a composite of aluminosilicate and magnesium bearing mineral phase. Traces of Fe, Ca, Na, K and Mn were also presence. These elements were present on the parent material before synthesis of the composite. Moreover, the composite is rich in base cations. Masindi et al. [33] reported that availability of base cations in solution aids in the removal of anions.

3.2. XRD analysis

The mineralogical composition for bentonite clay, magnesite and composite are presented in Figs. 1–3, respectively.

Fig. 1 shows that bentonite clay is characterized of Quartz, montmorillonite, calcite magnesian, magnetite, albite intermediate and muscovite. Fig. 2 shows that magnesite is dominated by periclase, brucite, monticellite and forsterite ferroan. This result corroborates results obtained by Nasedkin et al. [37] which state that crystalline/amorphous magnesite is constituted of greater than 90% of MgO. Fig. 3 shows that the composite is characterized of quartz, periclase, gibbsite, montmorillonite and muscovite. The results show that the composite is a combination of magnesite and bentonite clay. However, it is notable that there is an improvement in the chemical composition of the synthesized material. The obtained results corroborated results obtained by XRF analytical technique. Magnesium from magnesite and base cations from the clay matrices will aid in raising the pH of the solution and to scavenge boron from aqueous solution [21,35,38].

3.3. Brunet–Emmet–Teller analysis

The results for surface area and PZC for magnesite, bentonite clay and the composite are shown in Table 2.

Surface area is one of the most important aspects of adsorption. If the surface area is high, the adsorption capacity will also be high [5,7,8,21,35,38,39]. The BET surface area is the total of external surface area and micropore area. Bentonite clay has a surface area of 16.01 $m^2 g^{-1}$, magnesite has a surface area of 14.6 $m^2 g^{-1}$ and the composite has a surface area of 20.2 $m^2 g^{-1}$. Combination of magnesite and bentonite clay led to an increase in surface area of the composite. pH_{pzc} is one of the important parameter in adsorption. It dictates the type of species that will be adsorbed by the material at given pH. When pH_{pzc} is greater than the supernatant pH, the adsorbent will adsorb cations and when the pH of the supernatant is above the pH_{pzc}, the adsorbent will adsorb anions from the solution [3,5,35,38–41]. The pH_{pzc} value of a material is a reflection of the individual pH_{pzc} values of the components present. This shows that the composite will adsorb borate species from aqueous solution since it can raise the pH to greater than 11 [33].

Table 1
Elemental composition of bentonite clay, magnesite and the composite

% Composition	Bentonite clay	Magnesite	Composite before
SiO_2	66.51	4.76	51.72
Al_2O_3	16.81	0.14	10.37
Fe_2O_3	3.26	0.25	4.44
MnO	0.13	0	0.1
MgO	3.12	91.80	29.43
CaO	1.43	5.59	2.29
Na_2O	1.17	–	0.79
K_2O	0.54	0.003	0.32

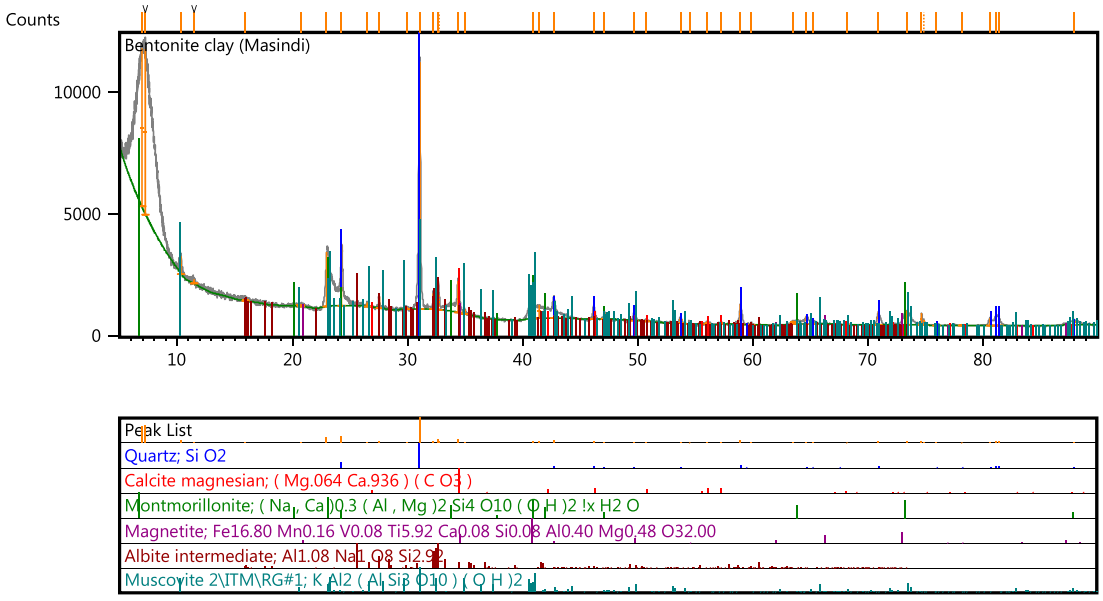

Fig. 1. Mineralogical composition of bentonite clay.

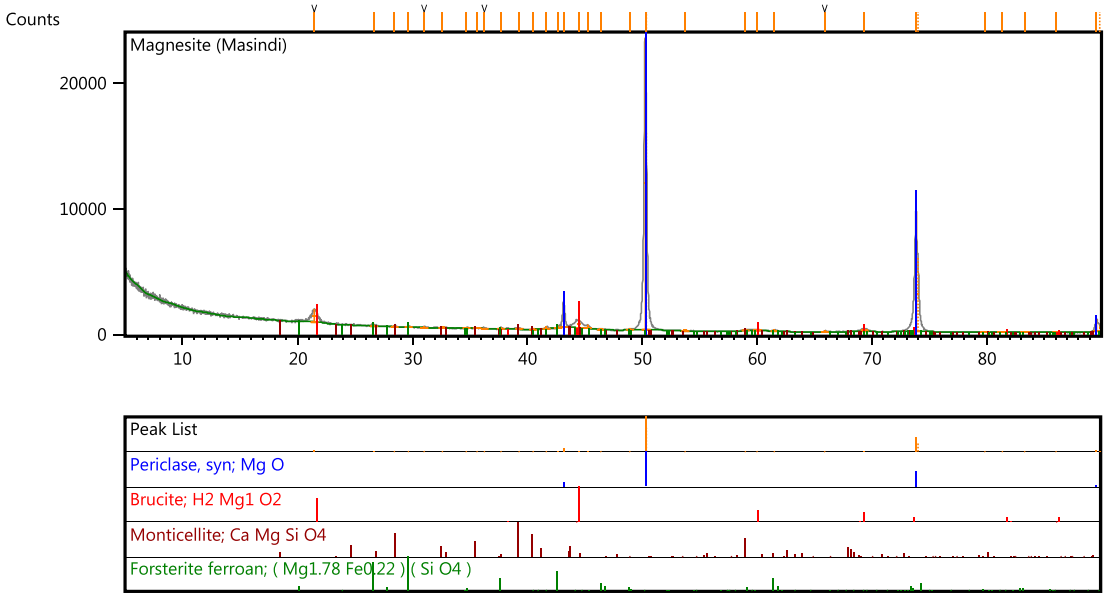

Fig. 2. Mineralogical composition of cryptocrystalline magnesite.

3.4. Optimization experiments

Several operational parameters were evaluated to configure optimum conditions for removal of boron from the aqueous solution. Effects of agitation time, dosage, concentration and pH were investigated.

Fig. 4(a) shows the effect of contact time on the equilibrium of boron adsorption onto the composite. The percentage removal of boron was observed to increase with an increase in contact time in the first 20 min. At 30 min, the system seems to have approached a steady state since no further change in adsorption was observed. Thereafter, the adsorption equilibrium curve levelled off throughout the investigation period. At 30 min, the system managed to remove 100% of boron from the solution. This study provided comparative results as compared to fly ash

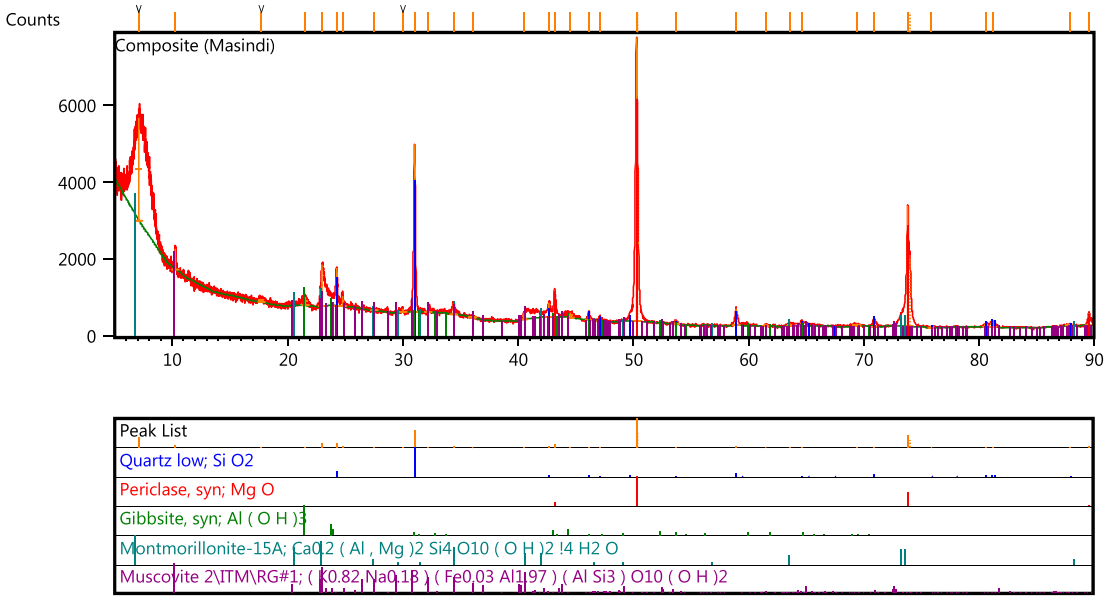

Fig. 3. Mineralogical composition of the composite.

Table 2
BET surface, micropore area, external surface area, micropore volume, total pore diameter and PZC of bentonite clay, magnesite and the composite

Parameter	Bentonite	Magnesite	Composite
BET surface area	16.01	14.6129	20.2
Micropore area	4.92	2.271	6
External surface area	11.08	12.3419	14.2
Micropore volume	0.0021	0.0009	0.003
Adsorption average pore diameter (4 V/A by BET)	74.07	222.9594	264
Point of zero charge (pH_{PZC})	8.1	8.5	10

that requires 24 h to remove boron from water [42]. The adsorption affinity of the composite to boron proved to be very high. This also provides evidence that the composite provided enough surfaces for sorption of those chemical species. At equilibrium, the synthesized material depleted all the boron species which were in solution. High percentage removal of boron may also be attributed to the presence of base cations of Mg^{2+}, Ca^{2+}, Na^{+} and K^{+} on the composite matrices. Those elements play an exceptional role in the adsorption of anions. Henceforth, it was concluded that 30 min of equilibration will be the optimum time for the removal of boron from aqueous solution.

In Fig. 4(b), the effect of composite dosage on boron removal is presented as percentage removal. The percentage removal of boron was observed to increase with an increase in the composite dosage. From 0.1 to 1 g, the removal of boron was drastic, thereafter, no significant change was observed. An increase in adsorption capacity of boron with an increase in dosage was attributed to more adsorption sites becoming available. One gram of composite dosage has provided enough surfaces for adsorption of boron from aqueous solution. This was shown by stabilization in percentage removal hence showing that the composite scavenged all the chemical species that were in aqueous solution. As such, the composite showed optimum removal efficiency at 30 min of equilibration and 1 g of composite dosage hence denoting that those conditions should be used in the subsequent experiments.

In Fig. 4(c), the effect of ion concentration on percentage removal of boron is presented as percentage removal and mg of boron adsorbed per gram of the composite. As depicted by Fig. 4(c), when the concentration of boron increases, the sorption capacity of the

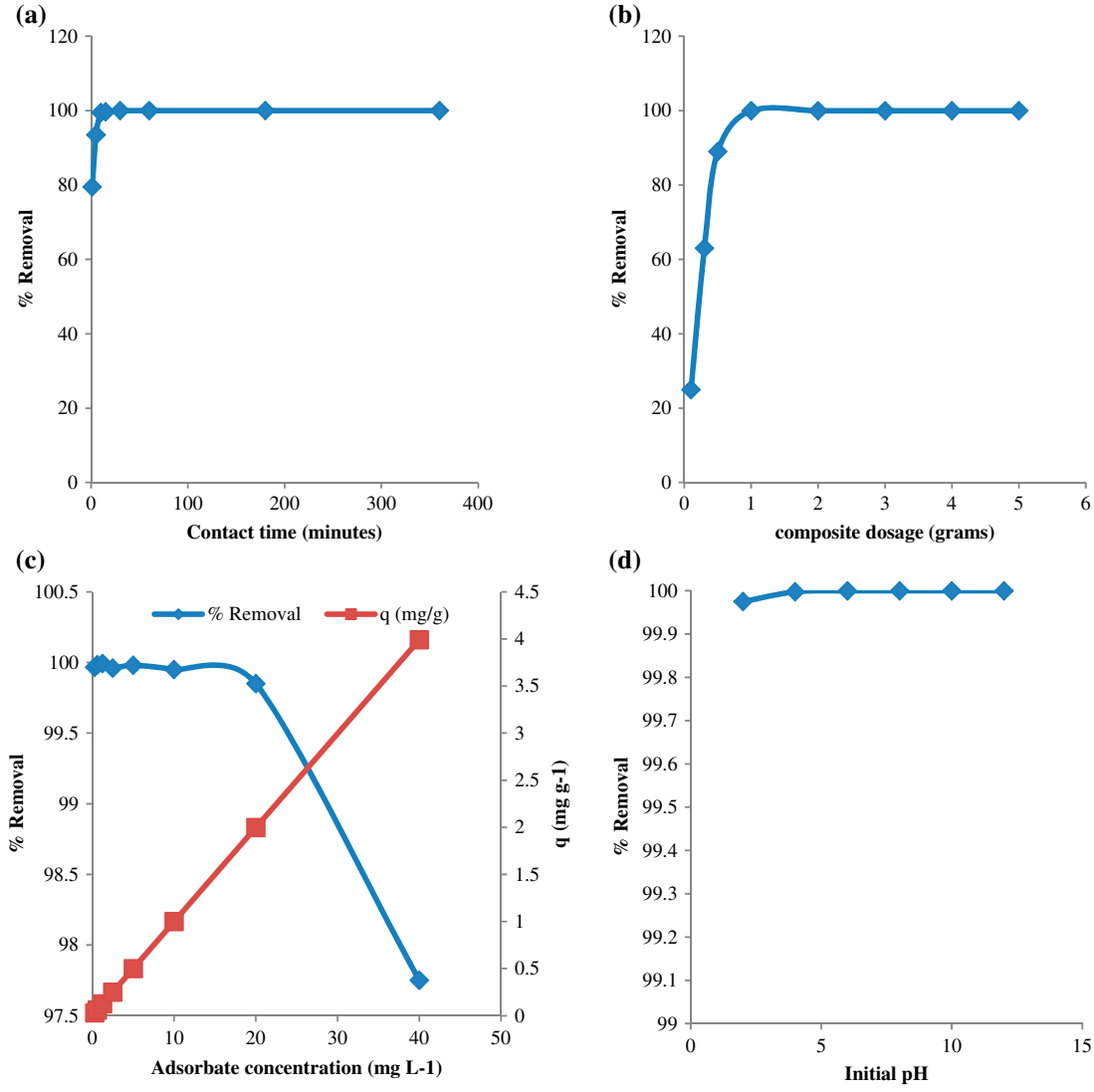

Fig. 4. Removal of boron from aqueous solution by varying time (0–360 min), dosage (0–5 g), ion concentration (0–40 mg L^{-1}) and pH (2–12) (250 rpm, pH 11, 1:100 S/L ratios and at ambient temperature).

composite gradually decreases. A decrease in adsorption percentage may be attributed to adsorption surfaces becoming finite as adsorbate concentration increases. More boron species are introduced to aqueous solution and the adsorption surfaces are becoming depleted. This also shows that the composite is becoming saturated with boron on its surfaces. At low concentration, more surfaces are available for adsorption of boron and at elevated concentration more surfaces are occupied with boron. Post 20 mg L^{-1}, the percentage removal of the composite was gradually going down. As such, it was concluded that 20 mg L^{-1} will be the optimum concentration of boron that can be removed by 1 g of the composite.

Fig. 4(d): the amount of boron adsorbed depends on the distribution of $B(OH)_3$ and $B(OH_4^-)$ which are controlled by the pH of the solution. The two species mainly compete for adsorption sites on the composite matrices. Due to leaching of the composite, the material releases base cations such as Mg^{2+}, Ca^{2+}, Na^+ and K^+. Those species play an exceptional role in elevating the pH of the counter solution and in adsorption of anions [35]. The elevated pH promotes the existence of $B(OH_4^-)$species [43]. Nevertheless, the point of zero charge (pH_{pzc}) of the composite plays a notable part in adsorption of boron species from aqueous solution. The pH_{pzc} of the composite has been established to be 11. If the value is above pH_{pzc}, the adsorber surfaces

are negatively charged and they are conducive for cation adsorption. If the value is below pH_{pzc}, the adsorber surfaces are positively charged and they are conducive for anion adsorption. Boron exists as $B(OH_4^-)$ and becomes a dominant species at pH 9–10 [43]. The pH of the solution is an important parameter in the adsorption process because it affects the solubility of the metal ion concentration of the counter ions on the functional groups of the adsorbent. From Fig. 4(d), it is shown that there is a sharp increase of adsorption from pH 2 to 6, after that the adsorption becomes steady. As pH increases, the composite adsorbs more boron onto its matrices since its rich in basic cations of earth alkali metals (Mg^{2+}, Ca^{2+}, Na^+ and K^+). When the composite is introduced to aqueous solution, it rapidly increases the pH of the solution hence creating conditions which favour the adsorption of boron. Moreover, it was concluded that from circumneutral to basic pH condition, the composite will be capable of scavenging boron from aqueous solution.

3.5. Adsorption isotherm

Adsorption parameters of boron adsorption onto the composite are shown in Fig. 5.

Adsorption parameters of boron adsorption onto the composite are shown in Table 3.

The results from isotherm modelling suggest that both Langmuir and Freundlich models fit the data better as shown by the correlation coefficient of 0.9543 for Langmuir and correlation coefficient is 0.9437 for Freundlich. This result demonstrates adsorption on both homogeneous and heterogeneous surface. The R_L value is between 0 and 1 hence showing that adsorption is favourable. The n value for Freundlich is within 1 and 10, thus proving that adsorption is favourable.

Table 3
Adsorption parameters for boron adsorption onto the composite

Adsorption isotherm	Value
Langmuir adsorption isotherm	
R^2	0.95
b	19
R_L	0.001
Q_m	4
Freundlich adsorption isotherm	
R^2	0.94
k	4.4
n	2.2

3.6. Adsorption kinetics

The high correlation obtained by plotting the linearized form of pseudo-second-order model ($R^2 = 1$) compared to that for the pseudo-first-order model ($R^2 = 0.7013$) demonstrated that the former gives a better fit, implying that the adsorption occurs via a chemisorption process. A plot of the linearized form of pseudo-second-order model (t/qt vs. t) is given in Fig. 6.

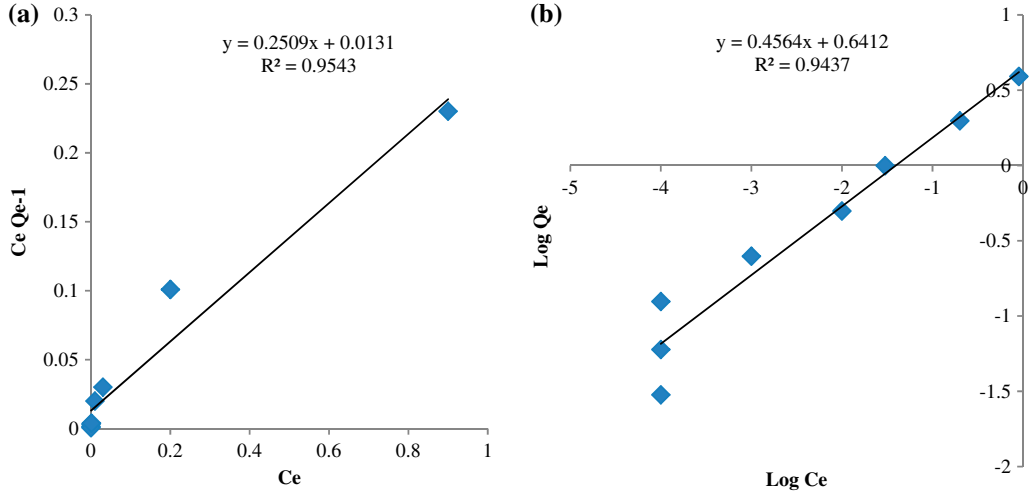

Fig. 5. The adsorption isotherm models: (a) the Langmuir isotherm model and (b) the Freundlich isotherm model. Reaction conditions: 30 min of equilibration, 1 g of the composite, 250 rpm, pH 11 and at ambient temperature. Boron concentrations were varied from 0.3 to 40 mg L^{-1}.

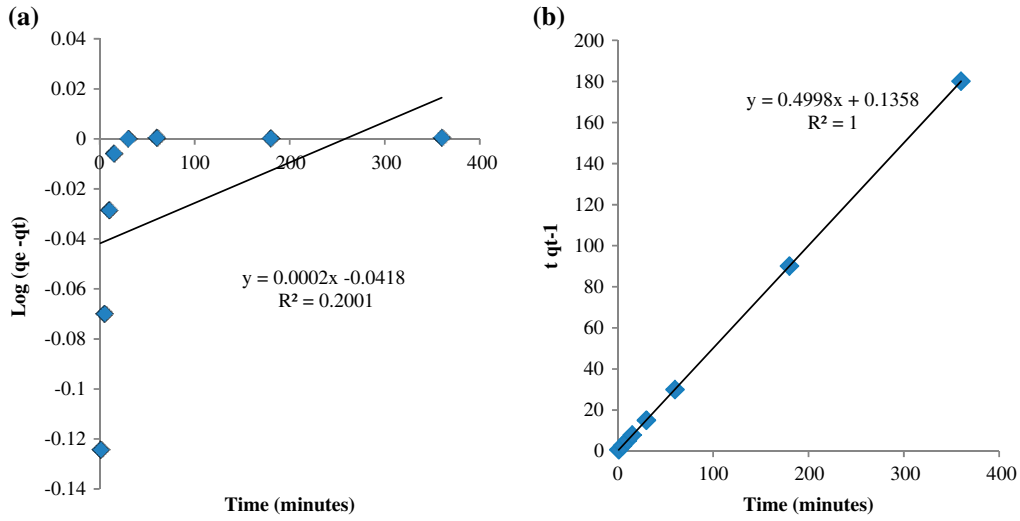

Fig. 6. The adsorption kinetic models: (a) the pseudo-first-order kinetic model and (b) the pseudo-second-order model. Reaction conditions: 1 g of the composite, 10 mg L^{-1} of boron, 250 rpm, pH 11 and at ambient temperature. Time was varied from 1 to 360 min.

Table 4
Comparison of adsorption capacities of materials used for removal of boron

Adsorbents	Adsorption capacity (mg g^{-1})	References
Fly ash agglomerates	0.014	[32]
The composite	4	Present study
Cryptocrystalline magnesite	1.34	Later study
SA bentonite clay	0.9	Later study
Activated carbon	0.09	[1]
Siral 5	1.12	[11]
Siral 40	0.97	[11]
Siral 80	0.94	[11]
Camlica Bentonite 1(CB2)	2.53	[44]
Camlica Bentonite 2(CB2)	0.12	[44]

3.7. Treatment of boron-rich effluent under optimized conditions

Removal of boron from wastewater using the composite was observed to be high and effective. The composite removed boron to below Department of Water Affairs and Forestry (DWAF) recommended water quality guidelines. Initially, the concentration of boron was 5 mg L^{-1} in mine leachates. After the treatment process, the level of boron was <0.01 mg L^{-1}.

3.8. Comparison of the present study with other adsorbents

A comparative study of different adsorbents for boron in contaminated water is shown in Table 4.

As shown by the table above, the composite offers best adsorption capacity for boron as compared to other adsorbents. The composite also showed improved adsorption for boron as compared to parent materials (magnesite and bentonite clay). This proves that the composite can be used as an alternative technology in position of conventional methods for treatment of boron.

4. Conclusion

The main conclusions of the present study are as follows:

(1) The composite can be successfully used for boron removal from industrial effluents.

(2) Optimum adsorption conditions are coordinated between 30 min of equilibration, 1 g of dosage, 20 mg L^{-1} of boron and all pH ranges.
(3) The data generated from various studies can be used to design various treatment plants for removal of boron in boron-rich effluents.
(4) The process adopted is simple, economic, viable and convenient since it relies on locally available natural material.
(5) Adsorption isotherm fitted to both Freundlich isotherm and Langmuir adsorption isotherm hence confirming that adsorption is heterogeneous in nature (inner and outer sphere complexes).

Acknowledgments

The authors wish to convey their sincere gratitude to Research and Innovation Directorate, Department of Ecology and Resource management, School of Environmental Sciences, University of Venda, Council of Scientific and Industrial Research (CSIR), SASOL-INZALO, National Research Foundation (NRF) and Department of Science and Technology (DST) (DST/NRF) for funding this project.

References

[1] İ. Kıpçak, M. Özdemir, Removal of boron from aqueous solution using calcined magnesite tailing, Chem. Eng. J. 189–190 (2012) 68–74.
[2] Y. Cengeloglu, G. Arslan, A. Tor, I. Kocak, N. Dursun, Removal of boron from water by using reverse osmosis, Sep. Purif. Technol. 64 (2008) 141–146.
[3] D.L. Sparks, Environmental Soil Chemistry, Academic Press, San Diego, CA, 1995.
[4] H.M.E. Selim, D.L. Sparks, S.S.S.o.A. Meeting Physical and Chemical Processes of Water and Solute Transport/retention in Soils: Proceedings of a Symposium Sponsored by Divisions S-1 and S-2 of the Soil Science Society of America in Baltimore, MD, 18 to 22 October 1998, Soil Science Society of America, 2001.
[5] H.M. Selim, D.L. Sparks, Heavy Metals Release in Soils, Taylor & Francis, Lewis publisher, New York, NY, 2001.
[6] R.E. Hester, R.M. Harrison, R.S.o. Chemistry, Mining and its Environmental Impact, Royal Society of Chemistry, Chichester, 1994.
[7] R.M. Harrison, Introduction to Pollution Science, RSC Publishing, San Diego, CA, 2006.
[8] B.J. Alloway, Heavy Metals in Soils, Chapman & Hall, 1990.
[9] X. Zhu, J. Ni, J. Wei, X. Xing, H. Li, Destination of organic pollutants during electrochemical oxidation of biologically-pretreated dye wastewater using boron-doped diamond anode, J. Hazard. Mater. 189 (2011) 127–133.
[10] R. Zhou, L. Di, C. Wang, Y. Fang, J. Wu, Z. Xu, Surface functionalization of microporous polypropylene membrane with polyols for removal of boron acid from aqueous solution, Chin. J. Chem. Eng. 22 (2014) 11–18.
[11] M. Yurdakoç, Y. Seki, S. Karahan, K. Yurdakoç, Kinetic and thermodynamic studies of boron removal by Siral 5, Siral 40, and Siral 80, J. Colloid Interface Sci. 286 (2005) 440–446.
[12] J. Yuan, Q. Guo, Y. Wang, Geochemical behaviors of boron and its isotopes in aqueous environment of the Yangbajing and Yangyi geothermal fields, Tibet, China, J. Geochem. Explor. 140 (2014) 11–22.
[13] E. Yoshikawa, A. Sasaki, M. Endo, Removal of boron from wastewater by the hydroxyapatite formation reaction using acceleration effect of ammonia, J. Hazard. Mater. 237–238 (2012) 277–282.
[14] A.E. Yılmaz, R. Boncukcuoglu, M.T. Yılmaz, M.M. Kocakerim, Adsorption of boron from boron-containing wastewaters by ion exchange in a continuous reactor, J. Hazard. Mater. 117 (2005) 221–226.
[15] A.E. Yilmaz, R. Boncukcuoğlu, M.M. Kocakerim, A quantitative comparison between electrocoagulation and chemical coagulation for boron removal from boron-containing solution, J. Hazard. Mater. 149 (2007) 475–481.
[16] Z. Yazicigil, Y. Oztekin, Boron removal by electrodialysis with anion-exchange membranes, Desalination 190 (2006) 71–78.
[17] M. del Mar de la FuenteGarcía-Soto, E.M. Camacho, Boron removal by means of adsorption with magnesium oxide, Sep. Purif. Technol. 48 (2006) 36–44.
[18] E. Bilgin Simsek, U. Beker, B.F. Senkal, Predicting the dynamics and performance of selective polymeric resins in a fixed bed system for boron removal, Desalination 349 (2014) 39–50.
[19] B. Bandura-Zalska, P. Dydo, M. Turek, Desalination of boron-containing wastewater at no boron transport, Desalination 241 (2009) 133–137.
[20] N. Kabay, E. Güler, M. Bryjak, Boron in seawater and methods for its separation—A review, Desalination 261 (2010) 212–217.
[21] D.L. Sparks, D.L. Sparks, Environmental Soil Chemistry, Academic Press, San Diego, CA, 2003.
[22] M. Tagliabue, A.P. Reverberi, R. Bagatin, Boron removal from water: Needs, challenges and perspectives, J. Cleaner Prod. 77 (2014) 56–64.
[23] O.C. Türker, H. Böcük, A. Yakar, The phytoremediation ability of a polyculture constructed wetland to treat boron from mine effluent, J. Hazard. Mater. 252–253 (2013) 132–141.
[24] O.C. Türker, J. Vymazal, C. Türe, Constructed wetlands for boron removal: A review, Ecol. Eng. 64 (2014) 350–359.
[25] Y. Seki, S. Seyhan, M. Yurdakoc, Removal of boron from aqueous solution by adsorption on Al_2O_3 based materials using full factorial design, J. Hazard. Mater. 138 (2006) 60–66.
[26] M. Turek, P. Dydo, J. Trojanowska, A. Campen, Adsorption/co-precipitation—Reverse osmosis system for boron removal, Desalination 205 (2007) 192–199.
[27] N. Öztürk, D. Kavak, T.E. Köse, Boron removal from aqueous solution by reverse osmosis, Desalination 223 (2008) 1–9.

[28] A.E. Yilmaz, R. Boncukcuoğlu, M.M. Kocakerim, M.T. Yilmaz, C. Paluluoğlu, Boron removal from geothermal waters by electrocoagulation, J. Hazard. Mater. 153 (2008) 146–151.
[29] T. Itakura, R. Sasai, H. Itoh, Precipitation recovery of boron from wastewater by hydrothermal mineralization, Water Res. 39 (2005) 2543–2548.
[30] J. Wolska, M. Bryjak, Methods for boron removal from aqueous solutions—A review, Desalination 310 (2013) 18–24.
[31] I. Polowczyk, J. Ulatowska, T. Koźlecki, A. Bastrzyk, W. Sawiński, Studies on removal of boron from aqueous solution by fly ash agglomerates, Desalination 310 (2013) 93–101.
[32] S. Seyhan, Y. Seki, M. Yurdakoc, M. Merdivan, Application of iron-rich natural clays in Çamlica, Turkey for boron sorption from water and its determination by fluorimetric-azomethine-H method, J. Hazard. Mater. 146 (2007) 180–185.
[33] V. Masindi, M.W. Gitari, H. Tutu, M. De Beer, Application of magnesite–bentonite clay composite as an alternative technology for removal of arsenic from industrial effluents, Toxicol. Environ. Chem. 53 (2014) 1–17.
[34] E. Kumar, A. Bhatnagar, M. Ji, W. Jung, S.H. Lee, S.J. Kim, G. Lee, H. Song, J.Y. Choi, J.S. Yang, B.H. Jeon, Defluoridation from aqueous solutions by granular ferric hydroxide (GFH), Water Res. 43 (2009) 490–498.
[35] M.A. Vicente, A. Gil, F. Bergaya, Chapter 10.5—Pillared clays and clay minerals, in: B. Faïza, L. Gerhard (Eds.), Developments in Clay Science, Elsevier, Amsterdam, 2013, pp. 523–557.
[36] D.W. Zachmann, W. Johannes, Cryptocrystalline magnesite, in: P. Möller (Ed.), Magnesite: Geology, Mineralogy, Geochemistry, Formation Mg-Carbonates (Monograph Series on mineral deposits, 28), Gebrüder, Berlin, 1989, pp. 15–28.
[37] V.V. Nasedkin, M.T. Krupenin, Y.G. Safonov, N.M. Boeva, S.V. Efremova, A.I. Shevelev, The comparison of amorphous (cryptocrystalline) and crystalline magnesites, Mineralia Slovaca 33 (2001) 567–574.
[38] H.M. Selim, W.L. Kingery, Geochemical and Hydrological Reactivity of Heavy Metals in Soils, Taylor & Francis, UK, 2003.
[39] D.L. Sparks, Kinetics of Soil Chemical Processes, Academic Press, UK, 1989.
[40] H.M. Selim, M.C. Amacher, Reactivity and Transport of Heavy Metals in Soils, Taylor & Francis, UK, 1996.
[41] I.L. Pepper, C.P. Gerba, M.L. Brusseau, Environmental and Pollution Science, Elsevier, San Diego, CA, 2011.
[42] C. Zhang, L. Chen, T.-J. Wang, C.-L. Su, Y. Jin, Synthesis and properties of a magnetic core–shell composite nano-adsorbent for fluoride removal from drinking water, Appl. Surf. Sci. 317 (2014) 552–559.
[43] S. Venkatamohan, S.V. Ramanaiah, B. Rajkumar, P.N. Sarma, Removal of fluoride from aqueous phase by biosorption onto algal biosorbent Spirogyra sp.-IO2: Sorption mechanism elucidation, J. Hazard. Mater. 141 (2007) 465–474.
[44] S.S. Yoldas, S.M. Yurdakoc, M. Merdivan, Application of iron-rich natural clays in Camlica, Turkey for boron sorption from water and its determination by fluorimetric-azomethine-H method, J. Hazard. Mater. 146 (2007) 180–185.